PARAMETERS OF AN EXPLOSIVE GAS COMPRESSOR JET

Yu. N. Kiselev, K. L. Samonin, and B. D. Khristoforov UDC 533.9.07 + 535.231.6

Of the explosive units converting the energy of an explosion by storage into the energy of a high speed plasma jet, the highest jet velocities are achieved by using an explosive gas compressor (EGC) [1, 2]. The high energy of the EGC plasma jet permits its successful application to produce powerful radiation sources [3, 4], to generate strong shocks [5], and to heat-treat metal surfaces [6]. A theoretical analysis of EGC operation [7, 8] is as yet approximate because of the complexity of the two-dimensional flow in the combustion chamber and the strong influence of the radiation. And the experimental results refer mainly to such quantities as the maximal jet velocity and its total energy [9], which are inadequate for the analyses of specific problems.

The distribution of the specific energy and the density along the EGC jet length, as well as the radiation emitted upon deceleration of the jet by an obstacle, are investigated in this paper. An EGC with a combustion chamber in the form of a spherical segment with 80 mm radius of curvature and 96 mm base diameter was used. An impactor in the form of a 2-mm-thick aluminum plate was hurled with a total energy of 4.27 MJ by a hexogene charge pressed to a density of 1.71 g/cm^3.

The total energy of a plasma jet was initially determined by the method proposed in [9], and which was 57 kJ for the case of the EGC combustion chamber filled with air at normal density, i.e., it was 1.3% of the explosion energy. The mean velocity of the shock generated by the plasma jet in an 8 mm diameter tube was 31 km/sec, measured by ionization transducers on a 75-mm base.

The parameter distribution along the jet length was determined during impact of the jet on the obstacle 3. The test set-up is shown in Fig. 1. The plasma jet from EGC 1, bursting the thin Lavsan diaphragm, traverses a tube of 10 mm diameter and 40 mm length, into a glass vessel 2 evacuated to 0.1 Pa and is stagnated at its bottom. The jet mass flow rate on the boundary of the decelerated domain, its height, the pressure at the obstacle, as well as the brightness temperatures of the stagnation domain in a direction parallel and at 45° to the obstacle, and the radiation fluxes from the surface of the stagnation domain, were measured in tests.

The escape and deceleration of the plasma jet were recorded by an SFR-2M slit photorecorder. A typical photorecording is presented in Fig. 2. The scan was taken behind a violet filter with an effective wavelength of 432 nm and halfwidth 20 nm. The observation was through the side surface of the glass vessel *a* and through the mirror 6 at a 45° angle to the obstacle b and the glass window in the obstacle, c. The brightness temperatures were determined by photometric comparison of the brightness of the object under investigation and of the standard source ÉV-45 [5]. Fluctuations in the brightness in the jet moving at constant velocity (Fig. 2) were recorded during the slit photoscan of the escape of the plasma jet into the vacuum. Considering these fluctuations to move with the mass flow rates, the mass flow rate at the time of passage through the reflected shock front was determined by the slope of their image on the photoscan.

The pressure on the obstacle was measured by using three piezotransducers 4 at different distances from the center of the obstacle. The transducers were calibrated with an air shock with a 10 MPa pressure before the test. The time resolution of the piezotransducer was 0.3 μsec.

The density in the incoming jet was determined from the relationship $\varphi = p/V(V + D)$ by the results of measuring the pressure p at the obstacle, the jet velocity V, and the reflected wave front D. The accuracy of such a method will be the higher, the more quasistationary the reflection process. Pressure drops in the shock-compressed layer because of the escape

Moscow. Translated from Zhurnal Prikladnoi Mekhaniki i Tekhnicheskoi Fiziki, No. 3, pp. 75-81, May-June, 1981. Original article submitted April 16, 1980.

0021-8944/81/2203-0354$07.50 © 1981 Plenum Publishing Corporation

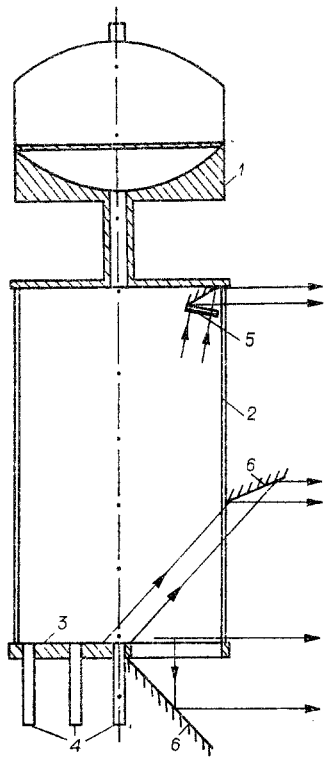

Fig. 1

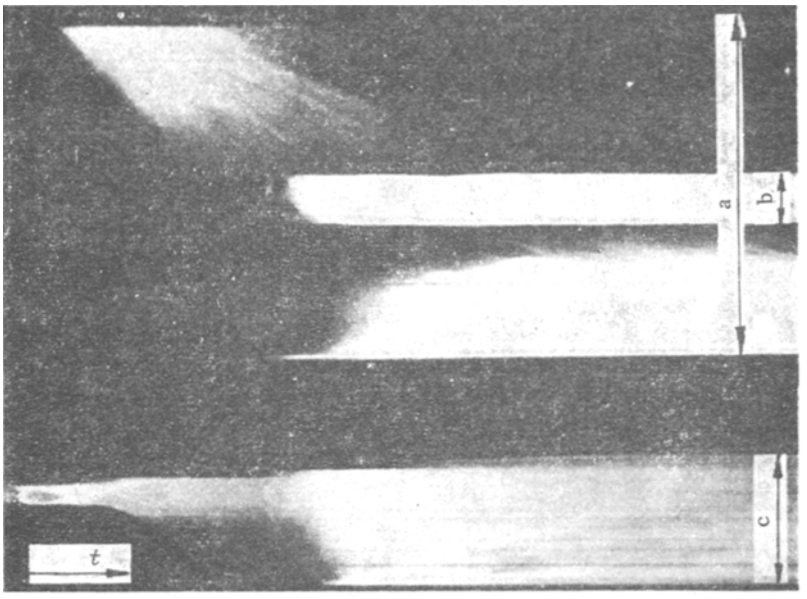

Fig. 2

of obstacle vapors are insignificant according to computations [10]. Analogy with a strong plane explosion shows that upon jet impingement with abrupt velocity and density drops, the pressure at the obstacle is not less than 40% of the frontal value.

The radiation fluxes emitted by the stagnation domain were measured by using a control glass plate 5 with aluminum strips of known thickness superimposed on its surface. Under the action of powerful radiation, evaporation and heating of the aluminum vapors occurs, and hence they become transparent in the visible spectrum range. Starting from the experimental dependences of such "burning through" of the aluminum from the incident radiation energy [4], and considering that the emitter is an equally-bright disk, the mean radiation fluxes from the surface of the decelerated domain during the burn-through of one aluminum strip were determined from the "burn-through" time and the location of the plate relative to the emitter.

Initially 0.077 g of normal-density air was in the EGC combustion chamber in the first test. The jet flew into an evacuated space of 90 mm diameter and 156 mm length. Values of the mass flow rate in the jet, the pressure on the obstacle, and the height h of obstacle standoff from the shock are represented in Fig. 3a as a function of the time. The velocity of the leading part of the jet reached 64 km/sec in the axial direction, and 20 km/sec in the radial direction. The velocity of the reflected shock had a maximum value of 5.5 km/sec at a time of 2 μsec after jet impact on the obstacle, and later dropped to 3.5 km/sec. All three piezotransducers showed the identical pressure. It reached 0.022 GPa at t = 2 μsec, diminished smoothly to 0.005 GPa at t = 14 μsec, and then rose sharply to 0.3 GPa.

The time shift between the change in pressure on the shock front and the pressure on the obstacle measured in the test was taken into account in computing the density of the incoming jet by the shift in the value of the pressure at the time of sound wave passage over the thickness of the stagnation domain. The sound speed in the stagnation domain was taken from the table in [11]. Because of the smooth change in pressure after the maximum of the hydrodynamic flow, this accounting yields a correction of not more than 20% to the density. The density computed in this manner in the jet ahead of the shock front and the mass

$\left(m = S\int \varphi V dt,\ S \text{ is the area of the obstacle}\right)$ proceeding into the decelerated domain are

represented in Fig. 3b. It is seen that the density in the jet increases with time, but the

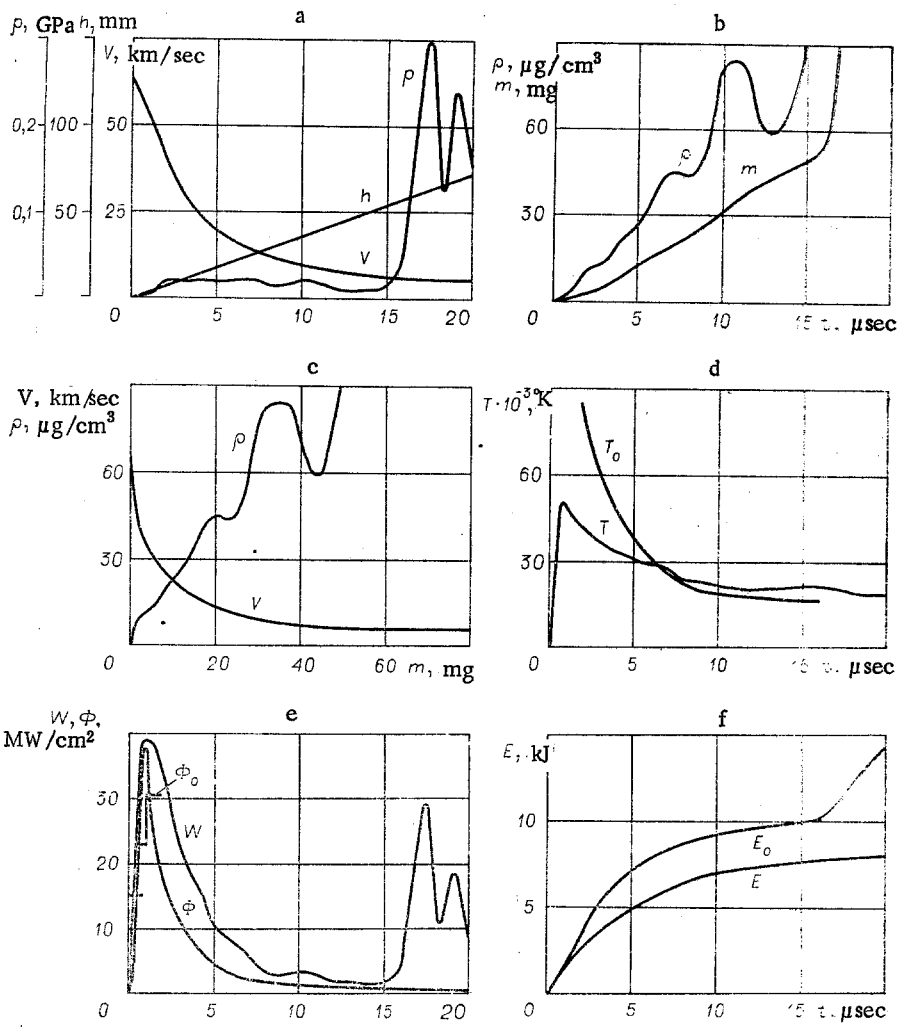

Fig. 3

TABLE 1

Test number	Gas	m_0, g	m_*, g	E_{0*}, kJ	E_*, kJ	$T_m \times 10^{-3}$ °K	W_m, MW/cm²	Φ_{cm}, MW/cm²
1	Air	0,077	0,032	9,1	7,0	50	39	31
2	Ne	0,053	0,10	14	5,2	39	36	17
3	Xe	0,35	0,017	2,0	1,2	28	1,9	—
4	Air	0,78	0,26	40	26	38	19	8,4

mass to 16 μsec is compared to the mass of gas initially in the EGC combustion chamber, and later increases abruptly. This permits the assumption that starting with this instant the dense part of the jet, moving at a 5-6 km/sec velocity and consisting mainly of material from the EGC combustion chamber walls (aluminum in our case), arrives.

It is seen from the velocity and density distributions over the jet mass that the EGC accelerates to a velocity above 10 km/sec half the initial mass of gas. A strong specific energy gradient in the mass exists in the highest velocity jet. A mass less than 0.002 g, i.e., around 2.5% of the initial mass of gas, possesses a specific energy of 1-2 MJ/g. A high-velocity jet possesses an energy of 9.1 kJ, which is 16% of the total jet energy. The rest of the energy belongs to the dense-low-velocity part of the jet.

An abrupt drop in the specific energy over the jet length also affects the radiative properties of the stagnation domain. The temperature T_0 that should be in the stagnation domain according to the shock adiabat of air [11], starting from the measured jet density

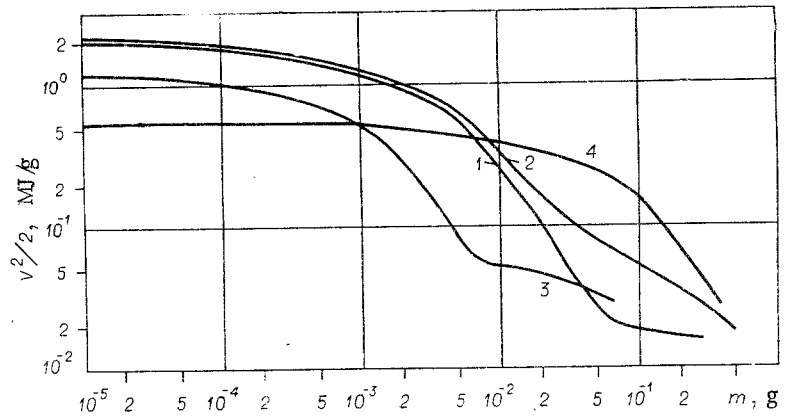

Fig. 4

and mass flow rate, is represented in Fig. 3d. The brightness temperature T measured at a 45° angle to the obstacle surface lies below to the time 6 μsec, and then later agrees with the temperature according to the shock adiabat. Values of the brightness temperature measured in a direction parallel to the obstacle lie still lower, which can be explained by the direct contact of the hot plasma on the glass wall in this direction. The radiation fluxes Φ from the surface of the stagnation domain, determined by using the control plate, and also the radiation fluxes Φ_o computed from brightness temperature measurements under the assumption of an absolutely black body, and the hydrodynamic energy flux $W = 0.5\varphi V^3$ coming into the stagnation domain, are given in Fig. 3d. The closeness of the measured and computed radiation fluxes indicates optical blackness of the emitter. The hydrodynamic energy flux reaches the maximum 39 MW/cm^2 1.5 μsec after jet impact on the obstacle. The maximum radiation flux measured by the control plate is 31 MW/cm^2, i.e., a significant part of the emitter jet energy. This and the abrupt drop in the hydrodynamic flux make recording high brightness temperatures impossible.

Under the assumption of an absolutely black emitter, the energy E emitted by the stagnation domain, which is represented in Fig. 3f, was computed by the brightness temperature distribution measured over the radiating surface. It is considered that the emitter is the surface of the cylinder without taking account of the obstacle surface. The hydrodynamic energy E_o being liberated in the stagnation domain is indeed presented in Fig. 3e. Effective conversion of the hydrodynamic energy occurs during deceleration of the high-velocity part of the jet. The efficiency of such a conversion diminishes with the arrival of the dense low-frequency part of the jet.

To determine the possibility of raising the efficiency of EGC operation, tests were performed with the compression chamber filled with neon and xenon at normal pressure, as well as with air at a pressure of 1.16 MPa. The results of all the tests are represented in the table, where m_o is the initial mass of gas in the compression chamber, m_* is the mass of jet with velocity $\geqslant 10$ km/sec, E_{o*} is the hydrodynamic energy belonging to the mass m_*, E_* is the energy radiated during the liberation of E_{o*}, T_m is the maximum brightness temperature, W_m is the maximum hydrodynamic flux, Φ_{om} is the maximum measured radiation flux. Distributions of the specific energy of 0.5 V^2 per mass of jet are also given in Fig. 4 for different compression chamber fillers. The numbers of the dependences correspond to the numbering of the tests in the table.

Tests showed that not only the density but also the kind of gas has substantial influence on EGC operation. Upon filling the EGC with neon, which is close to air in density, the specific energy distribution over the jet mass is close to the results of the first test for a jet mass less than 0.015 g. The remaining jet mass flies at considerably higher velocities than when the EGC is filled with air of normal density, which results in the ratio $m_*/m_o = 2$, i.e., in this case the jet is strongly "contaminated" by products of EGC wall evaporation under the effect of powerful shortwave radiation for which cold neon is transparent. The comparatively low radiation yield in this test can be explained by the strong shielding of the radiation by these impurities.

An increase in the density by filling the EGC compression chamber with xenon resulted in a substantial diminution in the operating efficiency of the EGC, the energy of the high-

velocity part of the jet was 2 kJ, and only 5% of the initial xenon mass was accelerated to a velocity greater than 10 km/sec. This is probably associated with the stronger heating of the xenon under shock compression in the EGC. The onset of the mass being evaporated from the wall becomes so strong here that the impactor stops without reaching the apex of the compression chamber. This also verifies the fact that the velocity of the jet being formed does not exceed 10 km/sec as the xenon mass is doubled by increasing the compression chamber volume by adding a cylindrical part.

Increasing the air density in the compression chamber by raising the pressure significantly equalizes the velocity distribution over the jet mass but with a reduction in the maximum velocity to 32 km/sec. The energy of the high-velocity part of the jet is here increased 4.4 times as compared to an air filler at normal density. For the jet density to approximate the density being realized in the first test, the plasma jet was expanded in this test in a flask of large size, of 142 mm diameter and 438 mm length. The radiation yield reached 25 kJ in 30 μsec.

The maximum radiation flux of 31 MW/cm^2 was measured in the first test. The temperature from the shock adiabat here considerably exceeds the measured value. Hence, by increasing the hydrodynamic flux because of a diminution in the jet escape to the side, the radiation flux from the stagnation domain can also be increased substantially. This follows also from the results of a numerical analysis of the problem of the impact of a jet of aluminum vapors of different density [10] which can be used for approximate estimates for air also because of the closeness of the radiation mean paths and the molecular weights.

Taking the above into account, it can be noted that a method to determine the density in a high-velocity jet by measuring the mass flow rate and pressure at an obstacle originating during stagnation of the jet is proposed and tested in this paper.

The specific energy distributions over the mass of an EGC jet are obtained for different gases filling the compression chamber. Strong growth of the density is noted for an abrupt reduction of the specific energy in the distribution over the mass of the EGC jet.

It is shown that not only the density but also the kind of gas substantially affects EGC operation. An increase in the density in the compression chamber by raising the air pressure considerably raises the efficiency of EGC operation because of equalization of the velocity distribution over the mass of jet. But a reduction in the maximum velocity of the jet occurs here.

The radiation yield, emitted during stagnation of the jet by the obstacle, is estimated from the measurement results. It is shown that as the jet stagnates, moving at velocities more than 10 km/sec, effective conversion of the jet hydrodynamic energy into radiation energy occurs. The coefficient of such a conversion can reach 0.6-0.7.

The authors are grateful to I. V. Nemchinov for constant interest in this paper and for useful discussions of the results.

LITERATURE CITED

1. A. E. Voitenko, "Obtaining high-velocity gas jets," Dokl. Akad. Nauk SSSR, 158, No. 6 (1964).
2. A. E. Voitenko, "Gas acceleration during compression under acute-angled geometry conditions," Zh. Prikl. Mekh. Tekhn. Fiz., No. 4 (1966).
3. A. E. Voitenko, E. P. Matochkin, and A. F. Fedulov, "Explosive lamp," Prib. Tekh. Eksp., No. 2 (1970).
4. Yu. N. Kiselev, B. D. Khristoforov, and M. A. Tsikulin, "Experimental investigation of the effect of power sources of continuous-spectrum radiation on an obstacle," in: Low-Temperature Plasma in Space and on Earth [in Russian], VAGO, Moscow (1977).
5. M. A. Tsikulin and E. G. Popov, Radiative Properties of Shocks in Gases [in Russian], Nauka, Moscow (1977).
6. V. I. Kirko, "Effect of a high-enthalpy plasma obtained by using an explosive source, on the inner surface of a cavity and a channel," Fiz. Goreniya Vzryva, 14, No. 6 (1978).
7. B. K. Crowley and H. D. Glenn, "Numerical stimulation of a high energy (Mach 120 to 40) air shock experiment," in: Proc. 7th Intern. Shock Tube Sympos., Univ. Toronto Press (1970).
8. G. S. Romanov and V. V. Urban, "Numerical modeling of an explosive plasma generator in a gasdynamic approximation," Inzh.-Fiz. Zh., 37, No. 5 (1979).

9. A. E. Voitenko and V. I. Kirko, "Efficiency of an explosive plasma compressor," Fiz. Goreniya Vzryva, 11, No. 6 (1975).
10. V. I. Bergel'son and I. V. Nemchinov, "On radiation occurring during impact of a gas layer on an obstacle at very high speeds," Prikl. Mekh. Tekhn. Fiz., No. 6 (1978).
11. N. M. Kuznetsov, Thermodynamic Functions and Shock Adiabats of Air at High Temperatures [in Russian], Mashinostroenie, Moscow (1965).

POSSIBILITIES OF AN EXPLOSIVE MHD GENERATOR AS AN ENERGY SOURCE FOR A PLASMA FOCUS

Yu. A. Burenin and G. A. Shvetsov

UDC 533.9;533.952.16

A plasma focus is presently one of the most powerful sources of neutron and x-ray radiation.

The analysis of experimental results shows that the neutron yield is $N \sim E_0^{\alpha} \sim I^{\beta}$, where E_0 and I are the discharge energy and current [1, 2], $1.5 \leqslant \alpha \leqslant 2.5$, and $\beta \sim 3.3$. Experiments have been conducted mainly with capacitor batteries having energies of up to 400 kJ. The use of explosive MHD generators, which make it possible to obtain a current and energy in the load exceeding their initial values by 10-50 times [3], is promising as the initial energy sources in the megajoule range.

Research on the electrotechnical matching of a specific explosive-magnetic generator with a plasma focus (EG-PF) was reported on in [4]. However, the explosive-magnetic generator under consideration, with a low inductance (400 cm) and a long working time (150 μsec) transferred a small fraction of its energy to the high-temperature plasma of the focus. In addition, the size of the chamber proved to be large: an outside diameter of 2.4 m and an insulator diameter of 90 cm. In the present report computer calculations are made modeling the operation of an explosive MHD generator loaded onto a noncylindrical Z pinch of N. V. Filippov's geometry [5]. The purpose of the work was to investigate the possibility of obtaining values of the current and energy in the plasma of the focus considerably exceeding the initial values of the current and energy in the generator and to determine the parameters of the EG-PF required for this. The motion of the current shell was described by the snowplow model [6]. As noted in [7, 8], the dynamics of the motion of a current shell far from the axis calculated from the snowplow model agrees with the experimental data and the results of two-dimensional MHD calculations. The relatively short duration of the last stage of cumulation of a shell, when the snowplow model is incorrect, should not significantly affect the matching of the times of EG and convergence of the shell. This is confirmed by the agreement between the experimental data and calculations from the snowplow model of a noncylindrical Z pinch supplied from a capacitor battery [9]. In accordance with experimental data on the neutron yield $N \sim E_0^{\alpha} \sim I^{\beta}$ we used two criteria for matching an explosive MHD generator with a plasma focus: obtaining the maximum density of kinetic energy E_k of the shell in the cumulation zone; obtaining the maximum current at the momemt of cumulation.

A diagram of an EG-PF system is given in Fig. 1. Because of axial symmetry the motion of the current shell is analyzed in the (r, z) plane. In Fig. 1, L_1 is the inductance of the generator, L_2 = const is the stray inductance of the circuit, R = const is the total resistance of the circuit, r_0 is the radius of the anode, z_1 is the height of the insulator, ρ is the gas density in the chamber, and **v** is the velocity of the shell. The operation of the system is described by the equations

$$\frac{\partial \mu}{\partial t} = 2\pi\rho r\left(v\frac{\partial r}{\partial \lambda} - u\frac{\partial z}{\partial \lambda}\right), \quad \frac{\partial(\mu u)}{\partial t} = -\frac{1}{c^2}\frac{I^2}{r}\frac{\partial z}{\partial \lambda}, \quad \frac{\partial(\mu v)}{\partial t} = \frac{1}{c^2}\frac{I^2}{r}\frac{\partial r}{\partial \lambda},$$
$$\frac{\partial r}{\partial t} = u, \quad \frac{\partial z}{\partial t} = v, \quad \frac{d}{dt}\left(\frac{L}{c^2}I\right) + RI = 0, \quad L = L_1 + L_2 + L_3, \tag{1}$$

Novosibirsk. Translated from Zhurnal Prikladnoi Mekhaniki i Tekhnicheskoi Fiziki, No. 3, pp. 81-86, May-June, 1981. Original article submitted April 7, 1980.

0021-8944/81/2203-0359$07.50 © 1981 Plenum Publishing Corporation